Journal of Applied and Numerical Analysis
2024, Vol. 2, pp. 18–29
doi: 10.30970/ana.2024.2.18

Evolutionary-numerical algorithm for unsteady inverse geometric problems in double-connected domains

I. Borachok

Ivan Franko National University of Lviv,
Universytetska Str. 1, 79000, Lviv, Ukraine

Анотація. Розглядається чисельне розв'язування задачі реконструкції внутрішньої межі двозв'язної області за відомими даними Коші на зовнішній частині області, для рівняння теплопровідності та хвильового рівняння. Обернена задача зводиться до мінімізації нелінійого функціоналу. Для мінімізації використовується дійснозначний генетичний алгоритм. Запропоновано оцінку індивіду, для обчислення якої потрібно розв'язати нестаціонарну задачу Діріхле. Для цієї задачі, спочатку виконується часткова дискретизація за часовою змінною, використовуючи метод Роте, а далі до отриманої послідовності стаціонарних неоднорідних рекурентних задач застосовується метод фундаментальних розв'язків. Запропонований підхід легко поширити на випадок вищих розмірностей, тому розглядаються двовимірні та тривимірні області. Алгоритм апробовано на декількох прикладах для обох рівнянь та стійкість методу підтверджена для вхідних даних із шумом.

Abstract. Numerical solution of the problem of reconstruction of the inner boundary of the double-connected domain from the given Cauchy data on the outer part of the domain, for the heat and wave equations is considered. The inverse problem is reformulated as a minimization of the nonlinear functional. A real-valued genetic algorithm is used for the minimization. A fitness function of the individual is proposed, for the calculation of which it is necessary to solve the non-stationary Dirichlet problem. For this problem, first a semi discretization by the time variable is performed using the Rothe's method, and then the method of fundamental solutions is applied to the obtained recurrent sequence of stationary inhomogeneous problems. The proposed approach is easy to extend to the case of higher dimensions, therefore two dimensional and three dimensional domains are considered. The algorithm is tested on several examples for both equations and the stability of the method is confirmed for the noised input data.

1 Introduction

Nondestructive techniques allow the inspection of an object's interior without causing damage. One such method is thermal or ultrasound medical imaging, which leads to inverse boundary value problems for the heat or wave equations, see [8, 14, 26] and references therein. In this context we are going to reconstruct the internal boundary of a medium from the Cauchy data given on the accessible part of the boundary.

More precisely, let D be a double-connected domain in $\mathbb{R}^d$, $d = 2, 3$, with the smooth boundary Γ consisting of two disjoint curves (or surfaces for $d = 3$) Γ_1 and Γ_2, both of class C^2, such that $\Gamma = \Gamma_1 \cup \Gamma_2$, $\Gamma_1 \cap \Gamma_2 = \varnothing$, Γ_1 is interior boundary and Γ_2 is exterior boundary. Firstly, let's consider the following forward (direct) initial boundary value problem for the heat equation. Find the bounded function u that satisfies

$$\begin{cases} \dfrac{1}{c}\dfrac{\partial u}{\partial t} = \Delta u & \text{in } D \times [0,T], \\ u = f_2 & \text{on } \Gamma_2 \times [0,T], \\ u = 0 & \text{on } \Gamma_1 \times [0,T], \\ u(\cdot,0) = 0 & \text{in } D, \end{cases} \tag{1.1}$$

Key words: non-linear inverse problem, wave equation, heat equation, boundary reconstruction, genetic algorithms, method of fundamental solutions.

where f_2 is a given sufficiently smooth function, $c > 0$ is a constant of the heat diffusivity, Δ denotes the Laplace operator and $T > 0$ is the final time. It is well known that there exists unique classical or week solutions, see [17,23].

Similarly, we formulate the forward problem for the wave equation. Find the bounded function u such that

$$\begin{cases} \dfrac{1}{\mathcal{C}^2}\dfrac{\partial^2 u}{\partial t^2} = \Delta u & \text{in } D \times [0,T], \\ u = f_2 & \text{on } \Gamma_2 \times [0,T], \\ u = 0 & \text{on } \Gamma_1 \times [0,T], \\ u(\cdot,0) = \dfrac{\partial u}{\partial t}(\cdot,0) = 0 & \text{in } D, \end{cases} \tag{1.2}$$

where $\mathcal{C} > 0$ is a given speed of sound. We refer to [24] on the well-posedness of the problem.

For both problems, the inverse problem is to determine the interior boundary Γ_1 from the additional measurement

$$\frac{\partial u}{\partial \boldsymbol{\nu}} = g_2 \quad \text{on } \Gamma_2 \times [0,T], \tag{1.3}$$

where g_2 is a given smooth function and $\boldsymbol{\nu}$ is the outward unit normal to the boundary Γ. The unknown interior boundary Γ_1 is uniquely identified by the Cauchy data (f_2, g_2) on the Γ_2, when $f_2 \neq 0$, see [12]. But the stability can't be guaranteed, see for example [22], therefore the regularization method is needed. In summary, we consider nonlinear ill-posed inverse problems for the heat equation (1.1), (1.3) and for the wave equation (1.2), (1.3).

In [11, 12] the inverse problem for the heat equation is interpreted as a nonlinear operator equation, that is solved by Newton's method, at each iteration the time-dependent direct problems are solved by the boundary integral equations method (BIEM). In [13] the inverse problem for the wave equation is reduced to the non-linear boundary integral equation, which is numerically solved using Newton's method and the BIEM. For both problems, impressive results have been obtained for two dimensional domains. The case of three dimensional domains is less studied due to the complex numerical algorithm of BIEM. There are several studies on three dimensional stationary problems, for instance the case for the Laplace equation, see [9, 18]. For recent research of the inverse problem for the heat equation in three dimensional, using the Newton's method and the method of fundamental solutions (MFS) with the time discretization, see [5].

This work is inspired by the research proposed in [19, 20], where the boundary reconstruction problems for the Laplace and Helmholtz equations are considered for two dimensional domains. As in the standard MFS, each solution of the problem is approximated by a linear combination of the fundamental solutions of the governing equation. Using the boundary conditions, the inverse problems are reduced to the minimization of the least-squares penalized functionals, with the subsequent application of the MatLab optimization solver.

We also interpret nonstationary problems as minimization problems, but instead apply a real-coded genetic algorithm (GA) for the numerical solution. GA is a stochastic optimization technique based on the laws of nature, see [25], which is often used when there is no classical numerical method or the existing method is very complex. In the GA potential solutions to the problems are represented as individuals in a population. For the selection purpose, a fitness function is computed for the each individual, which in our case requires the numerical solution of the corresponding direct problem. A two-step numerical method is used for the numerical solution of the direct problem: first, using the Rothe's method, the direct problem is reduced to a sequence of inhomogeneous problems for the modified Helmholtz equation, which is solved in the second step using the MFS, see [3,4,6]. MFS is a popular tool for the numerical solving of direct and inverse problems, especially for the elliptic equations, see [16,21], because it generates accurate results and requires less computational cost than BIEM.

The article has following structure: in section 2 we reduce the inverse problems to minimization problems and apply the GA. Computation of the fitness function, which requires the numerical solution of the direct problems is given in the section 3. For the direct problems, semi-discretization by the time and application of the MFS in the case of the sequence of stationary problems is developed also in the section 3. In the section 4, we present numerical results for both the heat and wave equations, as well as for two and three dimensional domains, which show the applicability of the proposed approach.

2 Application of the GA

There are several studies on the application of GA to inverse problems, for example, [7, 15], where GA with BIEM is used to numerically solve boundary reconstruction problem for the Laplace equation. The idea is to extend the methodology to the case of non-stationary problems.

For both inverse problems, suppose that the unknown interior boundary Γ_1 is a star-like curve (or star-like surface for $d = 3$) with respect to origin and has the following parametrization

$$\Gamma_1 = \begin{cases} \boldsymbol{\gamma}_r(s) = r(s)\boldsymbol{\omega}(s),\ s \in [0, 2\pi], & d = 2, \\ \boldsymbol{\gamma}_r(\theta, \varphi) = r(\theta, \varphi)\boldsymbol{\omega}(\theta, \varphi),\ \theta \in [0, \pi], \varphi \in [0, 2\pi], & d = 3, \end{cases} \tag{2.1}$$

where

$$\begin{cases} \boldsymbol{\omega}(s) = (\cos s, \sin s), & d = 2, \\ \boldsymbol{\omega}(\theta, \varphi) = (\sin\theta\cos\varphi, \sin\theta\sin\varphi, \cos\theta), & d = 3 \end{cases} \tag{2.2}$$

and r is the unknown radial function. Let's approximate r by the elements from a finite-dimensional subspace

$$r \approx \sum_{k=0}^{K} r_k \mathfrak{r}_k, \tag{2.3}$$

where $K \in \mathbb{N} \cup \{0\}$, $r_k \in \mathbb{R}$ coefficients to be determined and $\mathfrak{r}_k$ are basis functions. In two dimensional domains we use trigonometric polynomials basis $\mathfrak{r}_k$

$$\{1, \cos s, \sin s, \cos(2s), \sin(2s), \cos(3s), \sin(3s), \ldots\}$$

and in three dimensional domains we use real-valued spherical harmonics

$$\left\{Y^R_{0,0}(\theta,\varphi), Y^R_{1,-1}(\theta,\varphi), Y^R_{1,0}(\theta,\varphi), Y^R_{1,1}(\theta,\varphi), Y^R_{2,-2}(\theta,\varphi), Y^R_{2,-1}(\theta,\varphi), Y^R_{2,0}(\theta,\varphi), \ldots\right\},$$

where the real-valued spherical harmonics have the following representation

$$Y^R_{k,l}(\theta,\varphi) = c^l_k P^{|l|}_k(\cos\theta) \begin{cases} \cos(|l|\varphi), & l < 0, \\ 1, & l = 0, \\ \sin(|l|\varphi), & l > 0 \end{cases}$$

with coefficients $c^l_k = (-1)^{\frac{|l|-l}{2}} \sqrt{\dfrac{2k+1}{4\pi}\dfrac{(k-|l|)!}{(k+|l|)!}}$, and $P^{|l|}_k$ are associated Legendre functions of degree k and order $|l|$, see [1].

To find the coefficients r_k, we use the GA. The individual $\boldsymbol{r}$ is a vector of length $K+1$ with elements $\boldsymbol{r} = (r_0, \ldots, r_K)$. The individual's fitness function is constructed from the additional Neumann condition (1.3)

$$E(\boldsymbol{r}) = \left\| \frac{\partial u^{(r)}}{\partial \boldsymbol{\nu}} - g_2 \right\|^2_{L^2(\Gamma_2)} + \lambda \|\boldsymbol{r}\|^2_2, \tag{2.4}$$

where $u^{(r)}$ is the numerical solution of the direct problem for the heat (1.1) or wave (1.2) equations, when the inner boundary Γ_1 is given by the radial function r (2.3) with coefficients from the vector $\boldsymbol{r}$. Since the inverse problems are ill-posed, we need to include the regularization term $\lambda \|\boldsymbol{r}\|_2^2$, where $\lambda > 0$ is the regularization parameter. A numerical computing of (2.4) will be provided in the section 3.

The GA consists of the following steps:

1. Generate the initial population of individuals.
2. Evaluate the fitness function (2.4) for each individual in the population. If the stopping criteria is met, go to step 5, otherwise go to step 3.
3. From the current population, select individuals for reproduction based on their fitness.
4. Apply crossover and mutation operators to obtain new offspring. New offspring and elite individuals replace the current population. Go to step 2.
5. Select the best individual in the last population and use it as the desired vector $\boldsymbol{r}$ for approximation of the inner boundary Γ_1 in (2.3).

Let's consider these steps in more detail. The initial population is filled with individuals representing circles (or spheres for $d = 3$) of random radius: for each individual, we randomly generate the element $r_0 \in [R_{min}, R_{max}]$ and set all others $r_j = 0$, $j > 0$, where R_{min} and R_{max} are the minimum and maximum initial radii. The number of individuals in the population is fixed and configured by the parameter $pop_{size} > 0$.

In the second step, all individuals of the population are evaluated. The best $p_{el}\%$ individuals are copied unchanged to the new population; it's called elitism. This ensures that the quality of individuals in the population does not deteriorate. Other $(100 - p_{el})\%$ individuals are offspring. To create offspring, we select two parents using linear ranking [25] and apply crossover and mutation operators to the parents. This process continues until all $(100 - p_{el})\%$ children have been created. The new population replaces the current population and the iteration process continues.

In the linear ranking selection method, the population is sorted based on fitness values. The individual with the lowest fitness gets the highest rank 1, the second lowest gets rank 2, and so on, the last individual gets the rank pop_{size}. For each individual, we generate the probabilities

$$p_i = q - (rank_i - 1)\frac{2(pop_{size}q - 1)}{pop_{size}(pop_{size} - 1)},$$

with the selection pressure parameter $q \in \left[\dfrac{1}{pop_{size}}, \dfrac{2}{pop_{size}}\right]$ and $rank_i$ – the rank of the i-th individual. It's easy to see that $\sum\limits_{i=1}^{pop_{size}} p_i = 1$. After calculating the selection probabilities, individuals are selected using the roulette wheel selection method [25]. In general, linear ranking prevents the selection process from being dominated by individuals with extremely low fitness, helps maintain diversity in the population, and prevents premature convergence.

The crossover operator combines the genetic information of two parents. First, we check if the crossover will be applied, this is done based on the probability $p_c\%$, if so, we apply a uniform crossover, namely

$$\boldsymbol{r}_1^c = \alpha \boldsymbol{r}_1^p + (1 - \alpha)\boldsymbol{r}_2^p,$$
$$\boldsymbol{r}_2^c = (1 - \alpha)\boldsymbol{r}_1^p + \alpha \boldsymbol{r}_2^p,$$

where $\boldsymbol{r}_\ell^p$, $\ell = 1, 2$ are two parents, $\boldsymbol{r}_\ell^c$, $\ell = 1, 2$ generated two children and $\alpha \in (0, 1)$ is a random value.

The mutation operator introduces random changes to the individual. For this case, we also check whether the operator applies, based on the probability $p_m\%$. Then, we randomly select from

1 till 3 elements in the individual $\boldsymbol{r}$ and add random changes according to

$$r_i^m = S_m(B_i^r - A_i^r)r_i,$$

where r_i is the randomly selected element in $\boldsymbol{r}$, r_i^m – mutated element, S_m is a scaling constant and A_i^r, B_i^r – minimum and maximum admissible values for r_i.

As a stopping rule, we use the maximum number of iterations it_{max} and the maximum number of iterations it_{nc} of not improving of the best solution.

3 Numerical calculation of the fitness function

In this section, we describe the numerical computing of the fitness function (2.4). The inner boundary Γ_1 is given by the (2.1) and the coefficients r_k of the radial function (2.3) are taken from the individual $\boldsymbol{r}$. For the numerical solution of the initial boundary value problems (1.1) or (1.2) we will use the two-step numerical method, proposed in [3,4,6]. Let's briefly recall the main steps of the algorithm.

For both problems (1.1) and (1.2), the solution u is approximated by the sequence

$$u_n \approx u(\cdot, t_n),\ t_n = (n+1)h,\ h = \frac{T}{N+1},\ n = -1, 0, \dots, N,\ N \in \mathbb{N} \cup \{0\}, \tag{3.1}$$

where the elements u_n satisfy the sequence of elliptic problems with inhomogeneous right-hand side

$$\begin{cases} \Delta u_n - \mu^2 u_n = \sum\limits_{m=0}^{n-1} \beta_{n-m} u_m & \text{in } D, \\ u_n = f_{\ell,n} & \text{on } \Gamma_\ell,\ \ell = 1, 2, \end{cases} \tag{3.2}$$

where $f_{2,n} = f_2(t_n), f_{1,n} = 0$, $n = 0, \dots, N$, $u_{-1} = 0$, and for the heat equation: $\beta_n = (-1)^n \dfrac{4}{ch}$, $n = 1, \dots, N$, $\mu^2 = \dfrac{2}{ch}$, or for the wave equation: $\beta_1 = -\dfrac{2}{\mathcal{C}^2 h^2}$, $\beta_2 = \dfrac{1}{\mathcal{C}^2 h^2}$, $\beta_m = 0$, for $n = 3, \dots, N$, $\mu^2 = \dfrac{1}{\mathcal{C}^2 h^2}$. The sequence of problems (3.2) is obtained from the approximation of time derivatives by finite-difference approximations at mesh points t_n, see [10].

The functions u_n, $n = 0, \dots, N$ are approximated by the linear combinations of elements from the fundamental sequence

$$u_n(\boldsymbol{x}) \approx u_{n,M}(\boldsymbol{x}) = \sum_{m=0}^{n} \sum_{j=1}^{M} \alpha_{m,j} \Phi_{n-m}(\boldsymbol{x}, \boldsymbol{y}_j),\ \boldsymbol{x} \in D, \tag{3.3}$$

where $\boldsymbol{y}_j \notin \overline{D}$, $j = 1, \dots, M$ are selected source points and $\alpha_{m,j}$, $m = 0, \dots, n$, $j = 1, \dots, M$ are coefficients to be determined, $M \in \mathbb{N}$. The explicit expression for the elements of the fundamental sequence Φ_n are

$$\Phi_n(\boldsymbol{x}, \boldsymbol{y}) = \begin{cases} K_0(\mu|\boldsymbol{x} - \boldsymbol{y}|) v_n(|\boldsymbol{x} - \boldsymbol{y}|) + K_1(\mu|\boldsymbol{x} - \boldsymbol{y}|) w_n(|\boldsymbol{x} - \boldsymbol{y}|),\ \boldsymbol{x} \neq \boldsymbol{y}, & d = 2, \\ \dfrac{e^{-\mu|\boldsymbol{x}-\boldsymbol{y}|}}{|\boldsymbol{x} - \boldsymbol{y}|} \tilde{v}_n(|\boldsymbol{x} - \boldsymbol{y}|),\ \boldsymbol{x} \neq \boldsymbol{y}, & d = 3, \end{cases}$$

where K_0 and K_1 are modified Bessel functions, see [1], the polynomials v_n, w_n and $\tilde{v}_n$ are known, see [3,4].

By collocating on the boundary of the domain D, from the (3.2) we obtain the following recursive systems for determining the coefficients $\alpha_{n,j}$, for $n = 0, \dots, N$:

$$\sum_{j=1}^{M} \alpha_{n,j} \Phi_0(\boldsymbol{x}_{\ell,i}, \boldsymbol{y}_j) = f_{\ell,n}(\boldsymbol{x}_{\ell,i}) - \sum_{m=0}^{n-1} \sum_{j=1}^{M} \alpha_{m,j} \Phi_{n-m}(\boldsymbol{x}_{\ell,i}, \boldsymbol{y}_j),\ \ell = 1, 2, \tag{3.4}$$

where $\boldsymbol{x}_{\ell,i}$, $\ell = 1,2$, $i = 1,\ldots,\tilde{M}$ are selected collocation points, $\tilde{M} \in \mathbb{N}$. The recurrent systems (3.4) are obtained from the observation that only the coefficients $\alpha_{n,j}$ in front of Φ_0 have not been previously used in approximations $u_{0,M},\ldots,u_{n-1,M}$.

For two-dimensional domains, we assume that boundary curves are star-like curves with respect to origin and have following parametrization

$$\Gamma_\ell = \{\boldsymbol{\gamma}_\ell(s) = (\gamma_{\ell,1}(s),\gamma_{\ell,2}(s)), s \in [0,2\pi]\}\,,\ \ell = 1,2.$$

This parametrization is compatible with representation of Γ_1 in the (2.1). Then the source points are evenly distributed on the artificial curves by the following rule

$$\boldsymbol{y}_j = \begin{cases} \eta_2\boldsymbol{\gamma}_2(s_j), & s_j = \dfrac{4\pi}{M}j, & j = 1,\ldots,\dfrac{M}{2}, \\ \eta_1\boldsymbol{\gamma}_1(\tilde{s}_j), & \tilde{s}_j = \dfrac{4\pi}{M}\left(j-\dfrac{M}{2}\right), & j = \dfrac{M}{2}+1,\ldots,M \end{cases}$$

with $\eta_2 > 1$ and $0 < \eta_1 < 1$. Collocation points are placed on the boundary curves by the following rule

$$\boldsymbol{x}_{\ell,i} = \boldsymbol{\gamma}_\ell(s_i),\ s_i = \frac{2\pi}{\tilde{M}}i,\ i = 1,\ldots,\tilde{M},\ \ell = 1,2.$$

For three-dimensional domains, we assume that boundaries are star-shaped surfaces with following parametrization

$$\Gamma_\ell = \{\boldsymbol{\gamma}_\ell(\theta,\varphi) = (\gamma_{\ell,1}(\theta,\varphi),\gamma_{\ell,2}(\theta,\varphi),\gamma_{\ell,3}(\theta,\varphi)),\ \theta \in [0,\pi], \varphi \in [0,2\pi]\}\,,\ \ell = 1,2.$$

The source points are evenly distributed on the artificial surfaces by the following rule

$$\{\boldsymbol{y}_j\}_{j=1}^{M} = \{\tilde{\boldsymbol{y}}_{\ell,j_1,j_2}\}_{\ell=1,j_1=1,j_2=1}^{2,m_1,m_2} :\ \tilde{\boldsymbol{y}}_{\ell,j_1,j_2} = \eta_\ell\boldsymbol{\gamma}_\ell(\theta_{j_1},\varphi_{j_2}),$$

with $\theta_{j_1} = \dfrac{\pi}{m_1+1}j_1$, $\varphi_{j_2} = \dfrac{2\pi}{m_2}j_2$, for $j_1 = 1,\ldots,m_1$, $j_2 = 1,\ldots,m_2$, $\ell = 1,2$ and $M = 2m_1m_2$, for $m_1, m_2 \in \mathbb{N}$.

Collocation points are evenly distributed on the boundary surfaces Γ_ℓ, $\ell = 1,2$ by the following rule

$$\{\boldsymbol{x}_{\ell,i}\}_{\ell=1,i=1}^{2,\tilde{M}} = \{\tilde{\boldsymbol{x}}_{\ell,i_1,i_2}\}_{\ell=1,i_1=1,i_2=1}^{2,\tilde{m}_1,\tilde{m}_2} :\ \tilde{\boldsymbol{x}}_{\ell,i_1,i_2} = \boldsymbol{\gamma}_\ell(\theta_{i_1},\varphi_{i_2}),$$

with $\theta_{i_1} = \dfrac{\pi}{\tilde{m}_1+1}i_1$, $\varphi_{i_2} = \dfrac{2\pi}{\tilde{m}_2}i_2$, for $i_1 = 1,\ldots,\tilde{m}_1$, $i_2 = 1,\ldots,\tilde{m}_2$ and $\tilde{M} = \tilde{m}_1\tilde{m}_2$, for $\tilde{m}_1, \tilde{m}_2 \in \mathbb{N}$.

The ratio between the number of collocation and source points should be $2\tilde{M} \geq M$. For more information on source and collocation points distributions, see [2].

Finally, taking into account (3.1) and (3.3), we can compute the fitness function (2.4) by the following discrete rule

$$E(\boldsymbol{r}) = \sum_{n=0}^{N}\sum_{i=1}^{\tilde{M}}\left|\sum_{m=0}^{n}\sum_{j=1}^{M}\alpha_{m,j}^{(\boldsymbol{r})}\Psi_{n-m}(\boldsymbol{x}_{2,i},\boldsymbol{y}_j^{(\boldsymbol{r})}) - g_2(\boldsymbol{x}_{2,i},t_n)\right|^2 + \lambda\left\|\boldsymbol{r}\right\|_2^2,$$

where $\Psi_n(\boldsymbol{x},\boldsymbol{y}) = \dfrac{\partial\Phi_n(\boldsymbol{x},\boldsymbol{y})}{\partial\boldsymbol{\nu}(\boldsymbol{x})}$ and the coefficients $\alpha_{m,j}^{(\boldsymbol{r})}$ are obtained from the (3.4). Γ_1, given by the $\boldsymbol{r}$. We use the superscript $(\boldsymbol{r})$ next to the coefficients $\alpha_{m,j}$ and source points $\boldsymbol{y}_j$ to emphasize that they depend on the $\boldsymbol{r}$.

4 Numerical examples

In this section, the results of numerical examples of the reconstruction of the inner boundary for two and three dimensional domains for both unsteady problems are presented. In all examples, we generate synthetic data for a given boundary function $f_2(\boldsymbol{x},t) = t^2e^{-4t+2}|\boldsymbol{x}|$, by solving the appropriate direct problems (1.1) or (1.2), by the two-step MFS-based numerical method (section 3), and compute the Neumann trace g_2 on the outer boundary Γ_2. To avoid an inverse crime, we consider a larger number of source and collocation points compared to the inverse problem. In the case of noisy data, the noise is added to the function g_2, such that $\left\|g_2^\delta - g_2\right\|_{L_2(\Gamma_2\times[0,T])} \leq \delta$, where g_2^δ is the noised function and $\delta > 0$ is the noise level.

We use following parameters of the GA: population size $pop_{size} = 40$, crossover probability $p_c = 80\%$, mutation scaling $S_m = 0.1$, mutation probability $p_m = 50\%$, the number of elite individuals $p_{el} = 10\%$, selection pressure parameter $q = 0.0375$ $(1.5/pop_{size})$, max number of iterations $it_{max} = 200$ (or $it_{max} = 500$, for $d = 3$), max number of iterations without improvement $it_{nc} = 20$. The values of R_{min} and R_{max} depend on the knowledge of the minimum and maximum radii of the circles (or surfaces, for $d = 3$) allowed for the inner boundary, and we use neither too small nor larger than allowed so as not to exceed outer boundary, thus for $d = 2$ we use $R_{min} = 0.1$, $R_{max} = 0.6$ and for $d = 3$ we use $R_{min} = 0.1$, $R_{max} = 2$ (note that in front of $Y_{0,0}^R$ there is a coefficient c_0^0). A similar logic is used to select A_i, B_i and we use predefined decreasing modulo values: $A_i : 0, -0.3, -0.3, -0.2, -0.2, \ldots$, $B_i : 0.6, 0.3, 0.3, 0.2, 0.2, \ldots$ (for $d = 3$ we use $A_i : 0, -1.5, -1.5, -1.5, -1, -1, \ldots$, $B_i : 2, 1.5, 1.5, 1.5, 1, 1, \ldots$).

For numerical solution of the direct problem we use following parameters: $N = 10$, for $d = 2$: $M = 48$, $\tilde{M} = 24$, $\eta_2 = 2$, $\eta_1 = 0.5$ (when generate synthetic data g_2: $M = 96$, $\tilde{M} = 48$, $\eta_2 = 1.2$, $\eta_1 = 0.8$), for $d = 3$: $M = 72$, $\tilde{M} = 36$, $\eta_2 = 2$, $\eta_1 = 0.5$ (when generate synthetic data: $M = 128$, $\tilde{M} = 64$, $\eta_2 = 2$, $\eta_1 = 0.5$). In the case of small parameters, the fitness is calculated with an error, then for good individuals and bad individuals, similar fitnesses are obtained, this leads to a population with a large number of bad individuals and finding the wrong solution. On the other hand, when the parameters are too large, the fitness is calculated with a very small error for good individuals, but this increases the computational cost because we need to fill and solve the large recurrent systems for each individual for each population. Number of basis functions $K = 9$, for $d = 2$ and $K = 25$, for $d = 3$. The regularization parameter is chosen based on several numerical experiments, for which the most accurate result is obtained, namely $\lambda = 1e-10$, for $\delta = 0\%$ and $\lambda = 1e-4$, for $\delta = 5\%$. For the heat equation we use $c = 1$ and for the wave equation $\mathcal{C} = 1$, the final time is $T = 2$.

In examples 4.1 and 4.2 we show the results of numerical experiments in two-dimensional domains for the heat and wave equations, and three-dimensional domain for the heat equation is considered in the example 4.3.

Example 4.1. In this example we consider the inverse problem for the heat equation (1.1), (1.3) in two-dimensional domains. The exterior boundary curve Γ_2 is the unit circle

$$\Gamma_2 = \{\boldsymbol{\gamma}_2(s) = (\cos s, \sin s),\ s \in [0, 2\pi]\}$$

and the interior boundary curve Γ_1 (to be reconstructed) is an apple-shaped curve with the parametrization

$$\Gamma_1 = \left\{\boldsymbol{\gamma}_1(s) = \frac{1 + 0.9\cos s + 0.1\sin(2s)}{2 + 1.5\cos s}(\cos s, \sin s),\ s \in [0, 2\pi]\right\}.$$

The approximate curve was obtained after 200 iterations for exact data and after 150 iterations for noised data. In Fig. 4.1 the exact and reconstructed boundary curves Γ_1 are presented in the

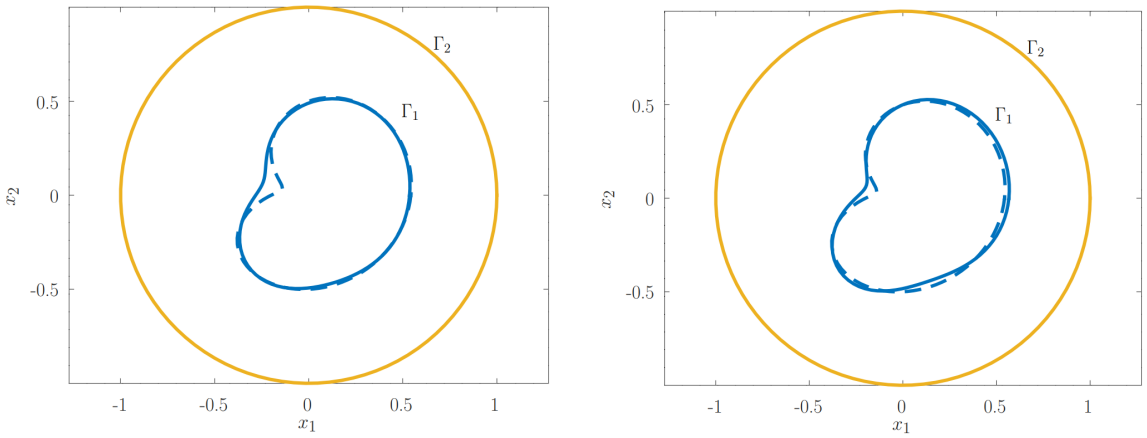

a) $\delta = 0\%$ b) $\delta = 5\%$

Fig. 4.1. Reconstructed (solid line) and exact (dashed line) boundary curves Γ_1 for exact and 5% noisy data for the heat equation for the example 4.1

case of exact (a) and noisy (b) data. The best fitness for every population is presented in fig. 4.2. It can be seen from this figure that quite good approximations are obtained in the first iterations, and the solution improves in the last iterations. The same tendency occurs for the case of the wave equation and three dimensional domains.

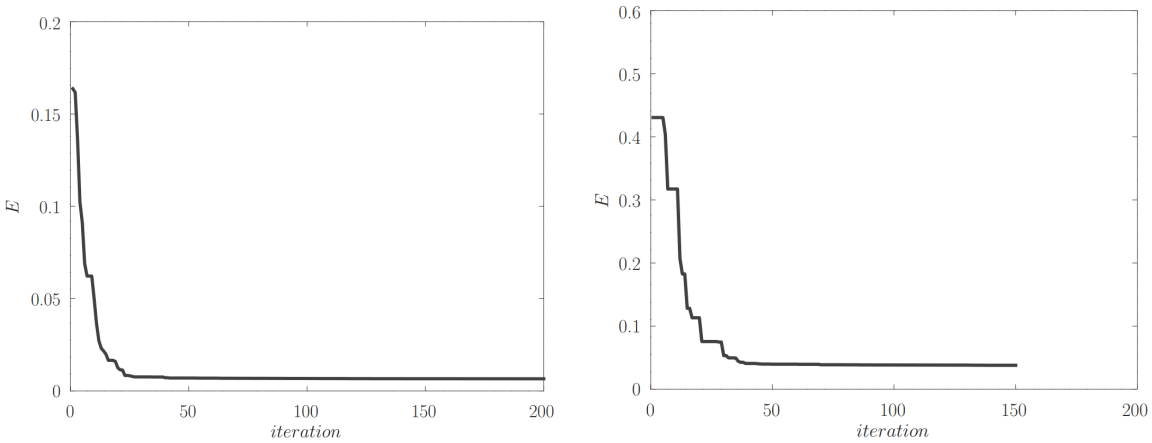

a) $\delta = 0\%$ b) $\delta = 5\%$

Fig. 4.2. The best fitness, computed by (2.4), for every population for the example 4.1

Example 4.2. In this example we consider the inverse problem for the wave equation (1.2), (1.3) in two-dimensional domains. The exterior boundary curve Γ_2 is a kite-shaped curve with the following parametrization

$$\Gamma_2 = \{\boldsymbol{\gamma}_2(s) = (\cos s, \sin s - 0.5\sin^2 s + 0.5),\ s \in [0, 2\pi]\}$$

and the interior boundary curve Γ_1 is a peanut-shaped curve with the parametrization

$$\Gamma_1 = \left\{\boldsymbol{\gamma}_1(s) = \sqrt{(0.5\cos s)^2 + (0.25\sin s)^2}(\cos s, \sin s),\ s \in [0, 2\pi]\right\}.$$

The approximate curve was obtained after 200 iterations for exact data and after 80 iterations for noised data. In Fig. 4.3 the exact and reconstructed boundary curves Γ_1 are presented in the case of exact (a) and noisy (b) data.

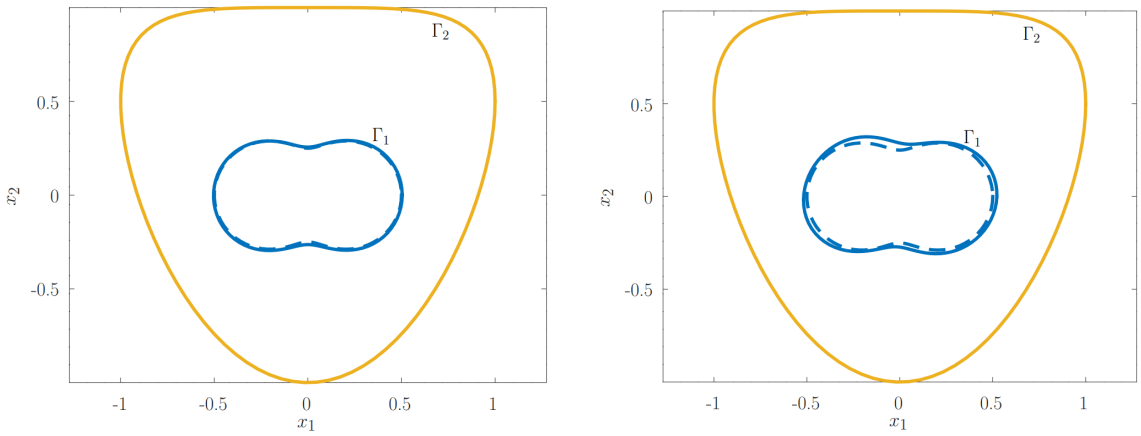

a) $\delta = 0\%$ b) $\delta = 5\%$

Fig. 4.3. Reconstructed (solid line) and exact (dashed line) boundary curves Γ_1 for exact and 5% noisy data for the example 4.2

Example 4.3. In this example we consider the inverse problem for the heat equation (1.1), (1.3) in three-dimensional domains. Boundary surfaces have following parametrization

$$\Gamma_2(\theta,\varphi) = \{\boldsymbol{\gamma}_2(\theta,\varphi) = \boldsymbol{\omega}(\theta,\varphi),\ \theta \in [0,\pi],\ \varphi \in [0,2\pi]\}\,,$$

$$\Gamma_1(\theta,\varphi) = \left\{\boldsymbol{\gamma}_1(\theta,\varphi) = \frac{1}{2}\sqrt{0.8 + 0.2(\cos(2\varphi)-1)(\cos(4\theta)-1)}\boldsymbol{\omega}(\theta,\varphi),\ \theta \in [0,\pi],\ \varphi \in [0,2\pi]\right\},$$

where $\boldsymbol{\omega}(\theta,\varphi)$ is given in (2.2).

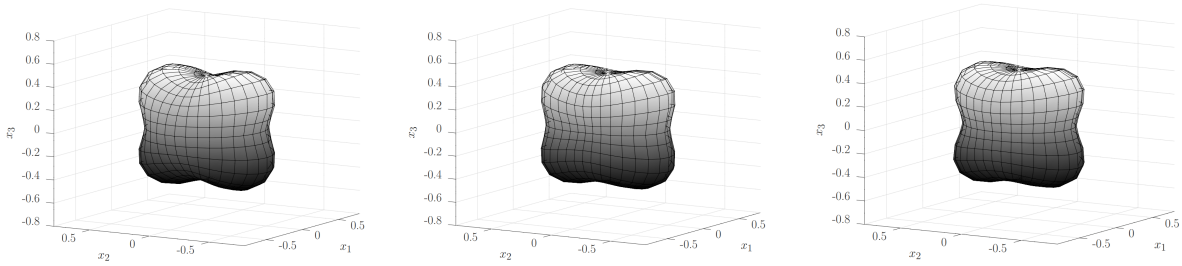

a) exact b) $\delta = 0\%$ c) $\delta = 5\%$

Fig. 4.4. Exact (a) and reconstructed boundary surfaces Γ_1 for exact (b) and 5% noisy (c) data for the example 4.3

The approximate surface was obtained after 500 iterations, and for noised data after 297 iterations. In Fig. 4.4 the exact and reconstructed boundary surfaces Γ_1 are presented; the sections of the domain at $x_1 = 0$ are presented in Fig. 4.5. Similar results are obtained in case of the wave equation. When the external boundary is more complicated the algorithm requires more iterations.

As can be seen from the results, in order to obtain an accurate numerical solution, it is necessary to perform a large number of iterations, especially for $d = 3$. For large values of M or $\tilde{M}$, the algorithm can work for a long time, so the optimal idea is to perform a small number of iterations by GA, and then refine the solution using Newton-type methods.

5 Conclusion

The application of GA is considered for the numerical solution of the inverse problem of reconstruction of the inner boundary of a double connected domain based on known Cauchy data of the

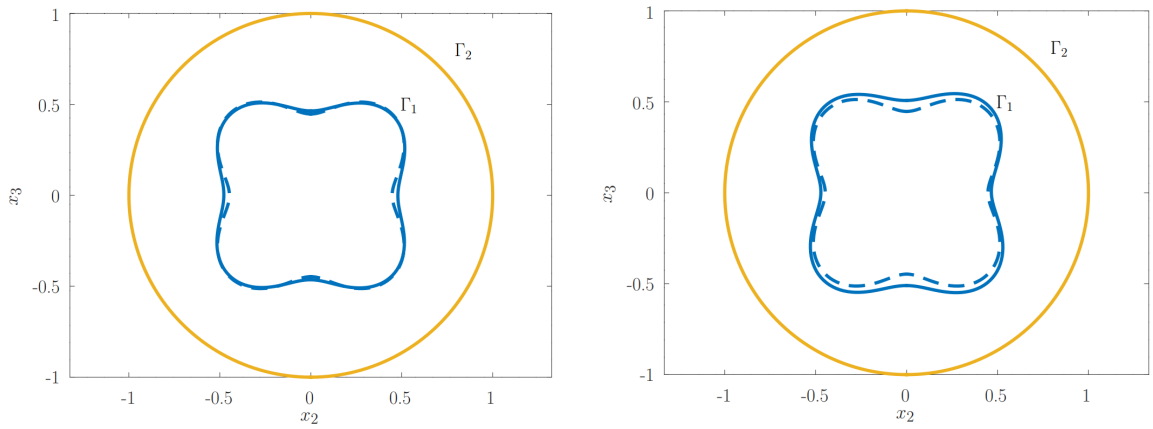

a) $\delta = 0\%$ b) $\delta = 5\%$

Fig. 4.5. Reconstructed (solid blue line) and exact (dashed blue line) sections of boundary surfaces Γ_1 at $x_1 = 0$, for exact and 5% noisy data for the example 4.3

function that satisfies either the heat or the wave equation. The radial function of the sought boundary is given in the form of the linear combination of basis functions, and the unknown coefficients are sought by GA. The fitness function of the individual is proposed, for the calculation of which it is necessary to solve a direct non stationary problem. The last problem according to Rothe's method is reduced to a sequence of recurrent stationary problems, which are completely discretized by the MFS. The algorithm is tested for both equations, for two and three dimensional domains, and for exact and noisy data. The advantage of the method is the possibility of application to other non stationary problems, and the lack of a good initial approximation, and the disadvantage is a large number of iterations in the case of complex domains, which can lead to a long execution time.

Declarations

Conflict of Interest.
The author has no conflict of interest to declare that are relevant to the content of this article.
Funding.
The work was supported by the DAAD Learnopolis+ program.
Author Contributions.
Not applicable.

References

1. Abramowitz, M., Stegun, I.A.: Handbook of mathematical functions with formulas, graphs, and mathematical tables. National Bureau of Standards Applied Mathematics Series, Washington, D.C. (1972)
2. Alves, C.J.S.: On the choice of source points in the method of fundamental solutions. Eng. Anal. Bound. Elem. **33**, 1348-1361 (2009)
3. Borachok, I., Chapko, R., Johansson, B.T.: A method of fundamental solutions for heat and wave propagation from lateral Cauchy data. Numer. Algorithms. **89**, 431-449 (2022)
4. Borachok, I., Chapko, R., Johansson, B.T.: A method of fundamental solutions with time-discretisation for wave motion from lateral Cauchy data. Partial Differ. Equ. Appl. **3** (37), (2022)

5. Borachok, I., Chapko, R.: A fundamental sequences method for an inverse boundary value problem for the heat equation in double-connected domains. Inverse Problems and Imaging. (2024) doi: 10.3934/ipi.2024043
6. Borachok, I.: On the method of fundamental solutions for the time dependent Dirichlet problems. Journal of Numerical & Applied Mathematics. **3**, 33-44 (2021)
7. Borachok, I., Marchenko, A.: Genetic programming for the two-dimensional boundary reconstruction problem. Visnyk Lviv Univ. Ser. Appl. Math. Comput. Sci. **31**, 127-141 (2023)
8. Chaji, K., Bagdouri, M.El., Channa, R.: A 2D domain boundary estimation. J. Phys. Conf. Ser. **135** (1), 012029 (2008)
9. Chapko, R., Ivanyshyn, O., Protsyuk, O.: On a nonlinear integral equation approach for the surface reconstruction in semi-infinite-layered domains. Inverse Probl. Sci. Eng. **21** (3), 547-561 (2012)
10. Chapko, R., Johansson, B.T.: A boundary integral equation method for numerical solution of parabolic and hyperbolic Cauchy problems. Appl. Numer. Math. **129**, 104-119 (2018)
11. Chapko, R., Kress, R., Yoon, J.: An inverse boundary value problem for the heat equation: the Neuman condition. Inverse Probl. **15**, 1033-1046 (1999)
12. Chapko, R., Kress, R., Yoon, J.: On the numerical solution of an inverse boundary value problem for the heat equation. Inverse Probl. **14**, 853-867 (1998)
13. Chapko, R., Mindrinos, L.: On the numerical solution of a hyperbolic inverse boundary value problem in bounded domains. Math. **10** (5), (2022)
14. Doubova, A., Fernández-Cara, E.: Some geometric inverse problems for the linear wave equation. Inverse Probl. Imaging. **9** (2), 371-393 (2015)
15. Eckel, H., Kress, R.: Non-linear integral equations for the complete electrode model in inverse impedance tomography. Appl. Anal. **87**, 1267-1288 (2008)
16. Fairweather, G., Karageorghis, A.: The method of fundamental solutions for elliptic boundary value problems. Adv. Comput. Math. **9**, 69-95 (1998)
17. Friedman, A.: Partial differential equations of parabolic type. Prentice-Hall, Englewood Cliffs, NJ (1964)
18. Ivanyshyn, O., Kress, R.: Identification of sound-soft 3D obstacles from phaseless data. Inverse Probl. Imaging. **4** (1), 131-149 (2010)
19. Karageorghis, A., Lesnic, D.: A meshless numerical identification of a sound-hard obstacle. Eng. Anal. Bound. Elem. **36** (7), 1074-1081 (2012)
20. Karageorghis, A., Lesnic, D.: Detection of cavities using the method of fundamental solutions. Inverse Probl. Sci. Eng. **17** (6), 803-820 (2009)
21. Karageorghis, A., Lesnic, D., Marin, L.: A survey of applications of the MFS to inverse problems. Inv. Pr. Sci. Engn. **19**, 309-336 (2011)
22. Klibanov, M., Rakesh: Numerical solution of a time-like Cauchy problem for the wave equation. Math. Methods Appl. Sci. **15**, 559-570 (1992)
23. Ladyzenskaja, O.A., Solonnikov, V.A., Uralceva, N.N.: Linear and quasilinear equations of parabolic type. American Mathematical Society, Providence, RI (1968)
24. Lions, J.L., Magenes, E.: Non-homogeneous boundary value problems and applications. Vol 2. Springer, Berlin (1972)
25. Michalewicz, Z.: Genetic algorithms + data structures = evolution programs. Springer, Berlin (1996)

26. Naik, N., Eriksson, J., de Groen, P., Sahli, H.: A nonlinear iterative reconstruction and analysis approach to shape-based approximate electromagnetic tomography. IEEE Trans. Geosci. Remote Sens. **46**, 1558-1574 (2008)

Received 07.10.2024
Revised 07.11.2024